2.1

Improved Representation of Cloud/Actinic Flux Interaction in Multiscale Photochemical Models

John N. McHenry, Carlie J. Coats
The Environmental Modeling Center at MCNC, Research Triangle Park, NC

1. INTRODUCTION

Processes which govern important surface photochemical reactivity include the interaction of clouds with solar radiation. At present, many photochemical models use algorithms that date from the 1980's, particularly those that are RADM-based (EPA-CMAQ, MCNC-MAQSIP, etc.). Recent evaluation demonstrates that the MAQSIP-RT forecast system has skill consistent with or better than the current statistical forecast tools for a New England Corridor ozone episode in August of 2001 (Ryan et al., 2003, these proceedings). However, summer 2001 forecast results showed a tendency toward over-forecasting ozone levels for moderate or marginal episodes. In particular, 15km-scale forecasts for the SE US and Texas revealed a high-bias on marginally polluted days. Combining feedback from operational forecasters with information gleaned from archived model runs, the authors concluded that deficiencies in the MAQSIP-RT-2001 actinic-flux/cloud-interaction sub-model were at least partly to blame. A thorough investigation of these deficiencies led to the design and implementation of a new, fast sub-model that treats the interaction of forecast clouds with solar actinic flux using improved science. This paper will describe the previously existing deficiencies, discuss the new sub-model, and present test results that show improvements in surface layer ozone predictions.

2. DESCRIPTION OF 2001 FORECAST MODEL AND ACTINIC FLUX SUB-MODEL

The photochemical model used in this study is the MAQSIP-RT (Multi-Scale Air Quality Simulation Platform–-Real-Time; McHenry, et al., 2000; McHenry et al., 2001). MCNC's North Carolina Supercomputing Center (NCSC) and the Pennsylvania State University (PSU) developed the initial operational version of this model as part of a joint Numerical Air Quality Prediction (NAQP) Project. It is currently operated as part of the South East Center for Mesoscale Environmental Prediction (SECMEP), a consortium of academic, public and private institutions. Details about the forecast models used and the projects they support are available at: http://www.emc.mcnc.org/projects/SECMEP.

The meteorological model is the PSU-NCAR MM5 version 3.4 (Grell et al., 1994). As configured during summer 2001, the MM5 used the Kain-Fritsch deep convection scheme (Kain and Fritsch, 1993) and a simple water/ice explicit moisture scheme (Dudhia, 1989). The soil model used was the default "slab" model with 5-layer heat diffusion. (Dudhia, 1996). The NCEP Eta model was used to initialize the MM5 with a 6-hour dynamic initialization of temperature, mixing ratio and wind components using analysis nudging except near the surface. The MM5 was configured with two domains using one-way nest interaction. The coarse grid covers most of North America at 45 km grid spacing (96 X 132) and the finer grid covers the eastern two-thirds of the United States at 15 km grid spacing (190 X 184). Typically the finer grid is spawned 6 hours into the coarse grid run, after spin up, with no nudging within the fine grid. There are 31 vertical layers in the model with 12-15 layers typically within the planetary boundary layer (PBL). The PBL scheme is the MRF-PBL (Hong and Pan, 1996). While there are a variety of PBL schemes available to the MM5 (e.g., Gayno et al., 1994; Burk and Thompson, 1989), the MRF-PBL is computationally very efficient and compared well in test runs. There appears to be a slight bias toward higher PBL heights with the MRF-PBL scheme. The newly developed shallow convection scheme is not used in the operational version (Deng et al., 1998).

During summer 2001, MAQSIP-RT used a modified Carbon Bond IV chemistry mechanism (Gery et al., 1989) along with the Bott flux form advection scheme (Bott, 1989). Vertical turbulent distribution of pollutants were determined using a K-theory scheme with predicted PBL heights provided by the MM5. Emissions were provided by the Sparse Matrix Operator Kernel Emissions (SMOKE) (Coats, 1995). The dry deposition module is incorporated into the code and follows Wesley, et al. (1985).

* *Corresponding author address*: John N. McHenry, Research Meteorologist, MCNC Environmental Modeling Center at the North Carolina Supercomputing Center. 3021 Cornwallis Road, Research Triangle Park, NC, 27709 mchenry@emc.mcnc.org

Clear-sky photolysis rate constant calculations, and their modification in the presence of forecast clouds, followed algorithms developed for the Regional Acid Deposition Model (RADM) (Chang et al., 1987) The approach used in the MAQSIP-RT utilized an off-line/on-line paradigm to calculate the rates. In the off-line step, the clear-sky actinic flux was calculated using a 2D (latitude-height) delta-Eddington radiative transfer model following Joseph et al. (1976). The actinic flux ***F(****l****)*** is defined as the spherical integral of the radiance $L(\lambda,\Theta,\phi)$:

$$F(l)=\int_{f}\int_{q} L(l,\Theta,f)\sin\Theta\, d\Theta\, df \quad (1)$$

where ϕ is the azimuth angle, Θ is the zenith angle, λ is wavelength, and the integral is taken over all angles. The calculation used six latitude bands (10^0N through 60^0N) and four heights (0m, 1000m, 3000m, and 10,000m ASL), for each hour from 0- through 9-hours-deviation from local noon on a standard summer day. This was driven by seasonal- or monthly-climatology vertical profiles of temperature, pressure, ozone, and aerosol concentrations. Reaction-specific data for absorption cross-section $\sigma_r(\lambda)$ and quantum yield $\varphi_r(\lambda)$ were inputs to the model, and rates (commonly referred to as "*J*-values") were calculated using a two-stream (direct, diffuse [downward and upward]) albedo-specific method for each photolytically active optical wave-band. The clear-sky rate coefficients can be expressed as:

$$j_r=\int_{l} s_r(l)\,j_r(l)\,F(l)\,dl \quad (2)$$

The online step then calculated each grid-cell's local solar time, and interpolated the clear-sky rates to the appropriate height and latitude, regardless of longitude. In the offline step, some attempt had been made to estimate the vertical profiles at about 90^0W longitude, or along a N-S plane through the eastern US. It then adjusted the clear-sky-interpolated rates for cloud effects using estimates of the cloud optical depth and the procedure outlined in Chang et al. (1987), in which the following fractional-sky-cover-based correction factor is applied:

$$j=(1-f_{cld})j_{clr}+f_{cld}R_{cld}j_{clr} \quad (3)$$

where j is the corrected photolysis rate, f_{cld} is the fractional cloud coverage, and R_{cld} is the ratio of the cloudy to clear-sky photolysis rates. Here, a parameterization was implemented in which R_{cld} was calculated as a function of solar zenith angle $\mu_0 \le 60^0$ and location either above, within, or below a single cloud layer:

$$R_{cld}=1+a_r(1-t_r)\cos m_0 \quad \text{(abv cld) (4a)}$$

$$R_{cld}=1.4\cos m_0 \quad \text{(within cloud) (4b)}$$

$$R_{cld}=1.6t_r\cos m_0 \quad \text{(below cloud) (4c);}$$

where α_r was a reaction-dependent coefficient given in Table 2 of Chang, et al. (1987), and the below-cloud transmissivity function t_r was parameterized as:

$$t_r=(5-e^{-t})/[4+3t(1-s_{ph})] \quad (5);$$

where τ is the cloud optical depth, and s_{ph} is a scattering phase function asymmetry factor assumed as 0.86 following Hansen and Travis (1974). Note that in this formula, when the optical depth is 0 (clear-sky), the transmissivity is unity.

In the original RADM, cloud optical depth was estimated using an approximation described in Stephens (1978):

$$t=3\bar{L}_{con}\Delta z_{cld}/2r_{H_2O}d_r \quad (6);$$

where $\bar{L}_{con}$ is the mean cloud liquid water content in g/m^3, Δz_{cld} is the depth of the cloud layer, r_{H2O} is the density of water, and d_r was an assumed mean cloud-droplet radius of 10^{-5} m.

Noting that estimation of clouds and their properties are uncertain, the authors focused substantial effort upon deficiencies in the online step of the calculation. Operationally however, the system was also severely limited by the offline step, because the clear-sky calculation was not integrated into the twice-daily operational forecast system, due to both complex data-flows and computational cost. "Typical summer-day" clear-sky photolysis rates, approximating solar-zenith angles and daylight duration in early July, had been saved in a look-up table and were being re-used irrespective of Julian date. This, combined with the built-in "hours-deviation-from-local-noon" approximation, was resulting in unacceptably large solar diurnal-cycle errors, over-estimating both the amount of daylight and the zenith-cosine for all days after about July 10^{th}.

It had been hoped, at first, that known deficiencies in the parameterization (3) – (6) would be amenable to a relatively simple fix. Previous research by the authors had discovered that (6), for example, tended to overestimate cloud optical depths, and that these overestimates could range

up to an order of magnitude larger than estimates given in Stephens (1978). In early versions of the MAQSIP model, this led to over-reduction in day-time photolysis rates given by (3) and a concomitant under-production of ozone.

A replacement for (6) had already been implemented in MAQSIP-RT and used operationally for several years, including the summer of 2001, in which the optical depth calculation followed Hansen (1983). In this scheme, a simple parameterization based on cloud type (convective versus non-convective) was borrowed from a global climate model. It was first utilized in the Seasonal Model for Regional Air Quality (SMRAQ) implementation of MAQSIP, where results showed the superiority of the MAQSIP cloud parameterization "in-toto" vis-a-vis the UAM-Vb approach. (Hogrefe, et al., 2001a, 2001b).

Nonetheless, the recognition that the model was systematically producing too much ozone on days that were only marginally polluted led to a revisitation of the Hansen (1983) formula. A comparison of optical depth calculations using the Hansen formula and the RADM equation (6) formula is shown in Figure 1, where the "new" label on the ordinate-axis indicates the Hansen formula, and the "old" label the RADM formula. By comparison, the optical depths for the non-absorbing wave-bands (0.3-0.75*um*) shown in Stephens (1978) Figure 1b, generally lie somewhere in the middle. This suggested that utilization of the Hansen (1983) formula could result in underestimates of cloud optical depths, and thus over production of ozone, on days when relatively thin cloud layers were suspected to be the difference between Code Yellow and Code Orange or Code Red peak 8-hour average ozone levels. The definition of the peak 8-hour average color codes used in ozone action day and health alerts by state forecasting agencies is provided below.

Further work suggested that the additional parts of the cloud-correction algorithm given by (4) and (5) were also relatively crude. For example, the below-cloud transmissivity function given in (5) is supposed to represent the fraction of light transmitted through the cloudy layer, emerging at cloud base, in a general sense. Comparison with delta-Eddington-based published transmissivities, in which the Joseph (1976) model was applied offline using clouds of varying optical depths (Madronich, 1987), and segregating between the direct and diffuse beams, showed that (5) most closely approaches the results for a direct beam at a solar zenith angle of 20^0, and that for other solar zenith angles, it overestimates the transmissivity. This too would contribute to over-estimation of below cloud photolysis rates--even with reliable optical depth calculations.

The problems with (4), (5), and (6) were then compounded when applied within the correction function (3). Properties of that function below cloud, in which (4c) is used to estimate R_{cld}, for a relatively high solar zenith angle of about 21^0, are shown as a function of different cloud fractional coverages in Figures 2 and 3. For ease of interpretation, the clear-sky *"J"* multiplication factor resulting from the following re-arrangement of (3) is depicted in the Figures:

$$j = j_{clear}[1 + f_{cld}(R_{cld} - 1)] \quad (7);$$

where the multiplication factor is in **[**].

Figure 2 shows that for optically thin clouds between 0.0 and 20.0, the function is not terribly sensitive to fractional coverage and has an inflection at an optical depth of about 8. Below this point, for clouds with optical depths between 5 and 8 at the given zenith angle, the multiplier is >1, resulting in "enhancements" above the clear-sky *"J"* values, up to a factor of 1.25. Madronich showed that such enhancements were theoretically possible, but observations using a ground-based actinometer (Jeffries, 2002, personal communication) *almost never saw such enhancements for any zenith angle*.

If the formula expressed in (3) and (7) is actually applied for even thinner clouds, the multiplier becomes even larger. Thus truncating the "effects of clouds" at an optical depth of 5 (a strategy used in RADM and propagated into MAQSIP-RT through the summer of 2001) was actually a means to prevent chemical rate-constant "blow-up" from occurring, due to the properties of (3) and (7). Pragmatically, this meant that for clouds with optical depths thinner than 5, clear-sky *"J"* was applied, but for clouds slightly thicker, up to an OD of around 8, enhanced clear-sky values were applied (for high zenith angles). Thus, thicker clouds (up to a point) resulted in greater photo-reactivity, a rather strange circumstance indeed!

For a wide range of optical depths, the properties of (7) are shown in Figure 3. Here, there is an exponential-asymptotic behavior in the function, varying according to fractional coverage, in which clouds with optical depths up to about 500, near the maximum of the range given in Stephens (1979), exert significant attenuation on the clear-sky values. This seems reasonable, but, given the added uncertainty in fractional coverage, the errors associated with other parts of the parameterization could either be amplified or cancelled.

Thus it became apparent that a simple fix was not possible. The combination of the two sources of error, one from the offline step, and one from the online step, led to a wholesale re-design of the

operational sub-model, which will be described in the next section.

3. DESCRIPTION OF IMPROVED ACTINIC FLUX—CLOUD–INTERACTION SUBMODEL

The new sub-model in the 2002 version of MAQSIP-RT corrects all of the problems discussed above, while implementing the "Simple Isotropic Model (SIM)" described in Madronich (1987). The SIM is implemented in the framework of MAQSIP-RT's multi-scale cloud package, which itself contains sub-models for deep and shallow convection, explicit clouds, and sub-grid scale non-convective clouds.

In the new sub-model, the older calculations in are re-partitioned, so that the *integral (2) is now calculated online* by reading in the components of the integrand in (2) as separate data-streams provided by a revised off-line module.

The revised offline module is now more highly discretized in the vertical, acting at 1000m increments up to 50,000m. The authors have found that extending the vertical depth of the offline module beyond its default 10,000m permits much more accurate estimation of clear-sky actinic radiation in MAQSIP-RT's upper layers, of importance for simulating the effects of stratospheric-tropospheric exchange and upper tropospheric chemistry.

In addition, the direct-downward, diffuse-downward, and diffuse-upward components of ***F(l)*** are now provided as separate radiative data streams to the online module. This allows the online module to implement the SIM. The product of the quantum cross-section times the quantum-yield is also provided by the offline module as a function of λ, reaction, and vertical level, in order to calculate (2) for each reaction.

The SIM was shown by Madronich (1987) to approximate the full delta-Eddington-with-clouds calculation to good accuracy. Wave-band specific albedos are brought into the online calculation in order to account appropriately for ground reflections in the SIM. By knowing the incident clear-sky direct and diffuse actinic fluxes at cloud-top, the SIM calculates the below and above cloud fluxes directly, obviating the need for (3)-(7). In-cloud actinic fluxes are calculated not by linear interpolation between the below- and above-cloud values, but by an interpolation weighted by layer-specific cloud-optical depth. This results in a de-facto resolution of multiply-layered clouds.

The downward integrated liquid water path *W* is used to determine the downward integrated cloud optical depth, using Stephens (1978) formula (10a) for conservative scattering. This calculation can be expressed as:

$$\log_{10}(t) = 0.2633 + 1.7095 \ln[\log_{10}(W)] \quad (8).$$

Stephens derived this equation by applying a full radiative transfer model using "standard" cloud types, valid for wavelengths of ~300-750nm, wherein conservative, non-absorbing scattering is a good approximation.

Furthermore, in-cloud albedos (and thus transmissivities) are now estimated for all appropriate solar zenith angles and for both direct and diffuse light, using a look-up table gleaned from values published in Madronich (1987). The Madronich values resulted from the cloudy application of the Joseph (1976) model. Thus, the cloud albedos vary as a function of solar angle in the revised model. For solar zenith angles greater than 60^0, the Chapman functions are implemented to account for light diffraction at low solar angles.

To correct the diurnal solar cycle problems, an accurate on-line calculation of the solar zenith angle applied to compute clear-sky rates was added, replacing the older "typical summer day" table look-up. This calculation was further linked with the SIM implementation, where it is needed to determine the conversion of direct to diffuse incident light. Readers should refer to Madronich (1987) for a description of the optical basis for this effect. In addition, a highly accurate (to within 5-minutes of published Naval Observatory values) sunrise/sunset-boundary algorithm was added so that the model turns on and off photochemistry at the correct local time for each grid cell.

To account for multiple cloud types in a single grid column, the SIM is implemented in two steps. The first step estimates the impact, if any, of explicitly resolved clouds in a grid column. Cloud top is determined as the location, proceeding down from the model top, where the integrated cloud optical depth exceeds a critical value, currently set at 5. We have found that for values <5, the SIM tends to predict below-cloud enhancement of clear-sky "*J*" more often than desired, but with less frequency than (7), and that above 5, it rarely predicts it. Cloud base is determined as that model level where the downward-integrated cloud optical depth reaches 99% of its total column value.

A corrector step is then made in which the same calculation is repeated, but for the *summed combination* of explicit plus convective/sub-grid clouds. Since the SIM does not know about fractional coverage, this calculation is done "as if" the combined cloud resided in the entire grid-column. Once the results of both steps have been calculated, the final SIM result is obtained by

weighting the predictor and corrector steps using the mean-cloud fraction above and below cloud base, and the individual layer-by-layer cloud fractions within the cloudy layers.

The mean cloud fraction is obtained by using the cloud vertical liquid water path as a weighting function. This represents the mean-cloud "shadow" below cloud base, and projection above cloud top. The procedure for calculating fractional coverage for the sub-grid scale clouds will be described elsewhere.

In summary, the new online module performs the following. For each advection time-step and horizontal grid cell, it computes the current local zenith cosine angle μ_0. If μ_0 is positive (i.e., if it is day-time instead of night at this cell and time-step), then it interpolates the three-component (direct, diffuse-downward, and diffuse-upward) clear-sky actinic radiation to the current latitude and zenith angle at all elevations in this cell's vertical column. The module does the same for the product of the quantum cross-section and quantum yield for each reaction. Then, it applies the SIM according to the procedure described, obtaining the revised above-cloud, in-cloud, and below cloud actinic fluxes for each albedo-specific waveband. The integral (2) may then be assembled directly, completely eliminating equations (3) though (7).

3. SOUTHEAST US TEST CASE, AUG 30, 2001

The new algorithms were tested in MAQSIP-RT using a forecast for August 30th, 2001, that was initialized at 1200UTC on Aug 29th. This forecast significantly over-predicted ozone in the southeast US.

Figure 4 shows visible satellite imagery valid at 1700UTC on Aug. 30th. As can be seen, a large swath of mid-high level moisture is in place over much of the area. The MM5 forecast predicted substantial cloudiness, as shown in Figure 5 below, in reasonable agreement with the imagery. The left-hand panel shows the new liquid-water-path-weighted *mean* fractional coverage, the right-hand panel the original non-weighted maximum-overlap fractional coverage. Both are similar in nature, but the optically thinner (thicker) clouds receive less (more) weight in the new scheme.

The observed clouds resulted in a relatively clean ozone day, as archived on the EPA AIRNOW Web-site (http://www.epa.gov/airnow), and shown in Figure 6. The only areas that reported values in the Code Yellow range (peak 8-hour concentrations between 65-84ppb) were in northern Florida and the Cincinnati suburbs. Most of the domain reported peak 8-hour average concentrations below 64ppb (Code Green).

Results of the modifications to MAQSIP-RT are shown in the next sequence of figures. Figure 7 shows a comparison of the below cloud correction factor applied to clear-sky photolysis rates in the new (left, 2002) versus the old (right, 2001) MAQSIP-RT. It is clear that the new algorithms make a substantial difference in the pattern and magnitude of the attenuation of the solar actinic flux. Large areas of the model domain are now subject to attenuation by factors of around 0.6, representing a 40% reduction in clear-sky values. Much of the domain in the old model was not affected by the forecast presence of clouds shown in Figure 5—with only the thickest of clouds (e.g. northern GA, central AL) resulting in effects. The patterns shown are generally representative of the whole day.

Figure 8 shows the difference (new left, old right) in sunset times resulting from implementation of the improved diurnal solar cycle computation (see explanation in figure caption). The new model correctly calculates the sunset time and shadow-angle, within 5 minutes of published values. Obviously, the RADM-based algorithm in the older MAQSIP-RT allowed photochemical reactions to occur much later in the evening—and earlier in the morning, than it should have, for much of the summer season. This would have contributed to over-predictions as the length-of-day error grew large.

The difference in forecast ozone values at 19:30UTC August 30th is shown in Figure 9. Here it is seen that the new model significantly improves over the old through reduction in ozone production. The peak value in the new model is 107PPB as opposed to 144PPB in the old model. Significant reductions at this hour are seen throughout AL, GA, SC, TN, and NC.

Figure 10 shows the 8-hour average ozone centered at 19:30UTC, comparing the old model (left) with the new model (right). In this figure, the color scales represent the EPA peak 8-hour average color code scales, with blue-to-green being 0-64ppb, yellow being 65-84ppb, orange being 85-104ppb, red being 105-124ppb, and purple being 125ppb and above. Most of the domain is now Code Green, the exception (Code Yellow) being parts of northern GA and small parts of western NC and eastern TN. In the old model, large areas of the domain were forecast Code Yellow (KY, VA, west-central NC, upstate SC, east TN, northern GA, and north-central AL), with smaller areas Code Orange (northern GA, parts of western NC, north-central AL, and northeast TN) and even Code Red (northern Atlanta suburbs).

5. DISCUSSION

There are a number of notable differences between the previous approach and the revised

one. The new algorithm uses *all relevant levels* in the input atmospheric data (MAQSIP-RT model top is at approximately 17,000m) instead of only a subset of the levels truncated at 10,000m, so that upper tropospheric photolysis rates are not significantly damped. The new algorithm *computes* clear-sky scattering in terms of the current simulation day's local time-step zenith cosine instead of this cell's midsummer-day "hours-from-local-noon." Consequently, the new algorithm computes more accurate photolysis rates even for clear-sky conditions, because it computes the radiation balance for the current time of the current simulation day, properly accounting for local sunrise/sunset times. In addition, the SIM implementation appears not to result in either unreasonable photolysis enhancement or diminution because it improves upon the science behind equations (3) through (7).

Overall, the approach used has demonstrated very promising results for the test case illustrated. The module was implemented in real-time in 2002. Preliminary results suggest a substantial improvement on marginally polluted days. Feedback from operational forecasters using the model during summer 2002 (Bridgers 2002; Harris 2002; Ryan 2002; Lambeth 2002) has been universally positive in this regard. Work is ongoing to compare statistically the 2002 performance against the 2001 performance.

Finally, the new approach creates a framework for improved analysis of the offline radiative transfer calculation and for incremental improvement in a modular fashion, including perhaps the following:

- Utilization of MM5 forecast meteorology to compute clear-sky actinic fluxes, by driving the offline model in real-time.
- Using forecast ozone and/or aerosols instead of monthly profiles for these variables. This would complete the feedback loop between ozone and the actinic flux that is heretofore (poorly) approximated.
- Using improved gridded wave-band-specific albedos.
- Integration into a unified meteorological/chemical model such as WRF-Chemistry.

Given the number and severity of errors described here, the authors have concern for all similar photochemical models, in particular those that have common pedigree and are being applied frequently for policy-making purposes.

ACKNOWLEDGEMENTS

The authors would like to thank Mr. Bob Cameron and the Texas Natural Resource Conservation Commission (TNRCC, now TCEQ) for partially supporting this work. We also acknowledge many helpful discussions with Don Olerud of the MCNC-EMC, and Harvey Jeffries of the UNC School of Public Health.

REFERENCES

Bridgers, George, 2002: Personal communication with authors. North Carolina Department of the Environment and Natural Resources, Division of Air Quality.

Bott, A., 1989: A positive definite advection scheme obtained by non-linear normalization of the advective fluxes, *Mon. Wea. Rev.*, **117**, 1006-1015.

Chang, J., et al.; 1987: A three-dimensional Eulerian and deposition model, Physical concepts and formulation, *J. Geophys. Res*., **92**, 14 681-14 700.

Chen F., and J. Dudhia, 2001: Coupling an advanced land-surface hydrology model with the Penn State/NCAR MM5 modeling . Part 1: Model implementation and sensitivity, *Mon. Wea. Rev*., **129**, 569-585.

Coats, C. J., Jr., 1995: High performance algorithms in the Sparse Matrix Operator Kernel Emissions (SMOKE) modeling system, Microelectronics Center of North Carolina, Environmental Systems Division, Research Triangle Park, North Carolina, 6 pp.

Deng, A., N. L. Seaman, and J. S. Kain, 1998: A parameterization for detraining cumulus-cloud mass into dissipating layer clouds, *Twelfth Conference on Numerical Weather Prediction,* Amer. Meteor. Soc., Dallas, 120-123.

Dudhia, J., 1996: A Multi-:Layer Soil Temperature Model for MM5. The Sixth PSU/NCAR Mesoscale Model Users' Workshop. Mesoscale and Microscale Meteorology Division, National Center for Atmospheric Research, Boulder, Co., 49-50.
'

Dudhia, J., 1989: Numerical study of convection observed during the winter monsoon experiment by a mesoscale three-dimensional model, *J. Atmos. Sci.*, **46**, 3077-3107.

Harris, Emily, 2002: Personal communication with authors. Arkansas Department of Environmental Quality.

Gery, M. W. et al., 1989: A photochemical kinetics mechanism for urban and regional scale computer models, *J. Geophys. Res.*, **94**, 12 295-12 356.

Grell, G. A., J. Dudhia, and D. R. Stauffer, 1994: A description of the fifth-generation Penn State/NCAR Mesoscale Model (MM5). NCAR Tech. Note, NCAR/TN-398+STR, 122 pp.

Hansen, J., G. Russell, D. Rind, P. Stone, A. Lacis, S. Lebedeff, R. Ruedy, and L. Travis, 1983: Efficient three-dimensional global models for climate studies: Models I and II. Mo. Weath. Rev. **111**, 609-662.

Hansen, J.E., and L.D. Travis, 1974: Light scattering in planetary atmospheres. *Space Science Review* **16**, 527-610.

Hogrefe, C., S.T.Rao, P. Kasibhatla, G. Kallos, C.J. Tremback, W. Hao, D. Olerud, A. Xiu, J. McHenry, and K. Alapaty, 2001a: Evaluating the performance of regional-scale photochemical modeling systems: Part I—meteorological predictions. *Atm. Env.* **35**, 4159-4174.

Hogrefe, C., S.T.Rao, P. Kasibhatla, W. Hao, G. Sistal, R. Mathur, and J. McHenry, 2001b: Evaluating the performance of regional-scale photochemical modeling systems: Part II—ozone predictions. *Atm. Env.* **35**, 4159-4174.

Hong, S.-Y., and H.-L. Pan, 1996: Nocturnal boundary layer vertical diffusion in a medium range forecast model, *Mon. Wea. Rev,,* **124**, 2322-2339.

Kain, J. S. and J. M. Fritsch, 1993: Convective parameterization for mesoscale models: The Kain-Fritsch scheme, *The Representation of Cumulus Convection in Mesoscale Models,* K. A. Emanuel and D. J. Raymond, Eds., American Meteorological Society, Boston, 246 pp.

Jeffries, Harvey, 2002: Personal Communication with Authors. University of North Carolina at Chapel Hill, School of Public Health.

Joseph, J.H., W.J. Wiscombe, and J.A. Weinman, 1976: The delta-Eddington approximation for radiative flux transfer. *J. Atmos. Sci*., 33, 2452-2459.

Lambeth, Bryan, 2002: Personal Communication with authors. Texas Natural Resource Conservation Commission, Monitoring and Operations Division.

Madronich, 1987: Photodissociation in the atmosphere: I. Actinic flux and the effects of ground reflections and clouds. *J. Geophys. Res.* **93**, D8, 9740-9752

McHenry, J. N., et al., 2000, The NCSC-PSU numerical air quality prediction project: Initial evaluation, status, and prospects, *Symposium on Atmospheric Chemistry in the 21st Century*, American Meteorology Society, Boston, 95-102.

McHenry, J. N., et al., 2001, High-Resolution Real-Time Ozone Forecasts for the August-September Texas AQS-2000 (Houston) Field Study: Forecast Process and Preliminary Evaluation. *A Millenium Symposium on Atmospheric Chemistry: Past, Present, and Future of Atmospheric Chemistry.* American Meteorological Society, Boston, 186-193.

Ryan, W. F., 2003: Use of Numerical Ozone Prediction Models in Operational Air Quality Forecasting. *Fifth Conference on Atmospheric Chemistry: Gases, Aerosols, and Clouds.* Feb 9-13. American Meteorological Society, Boston.

Ryan, W. F., 2002a: Air quality forecast report – Philadelphia forecast area, 2001, http://www.meteo.psu.edu/~wfryan/phl_2001_final_report.htm.

Ryan, W. F., 2002b: Summary of the 2001 mid-Atlantic ozone season, http://www.meto.umd.edu/~forecaster/episodes/summary2001_0222.htm.

Ryan, W. F., 2002c: Personal communication with authors. Department of Meteorology, The Pennsylvania State University.

Ryan, W. F., C. A. Piety, and E. D. Luebehusen, 2000: Air quality forecasts in the mid-Atlantic region: Current practice and benchmark skill, *Wea. Forecasting*, **15**, 46-60.

Stephens, G.L., 1978: Radiation profiles in extended water clouds. *J. Atm. Sci* **35**, 2123-2132.

Wesely, M.L., D.R.Cook, R.L.Hart, and R.E. Speer, 1985: Measurements and parameterization of particulate sulfur dry-deposition over grass. *J. Geophys. Res.*, **90**, 2131-2143.

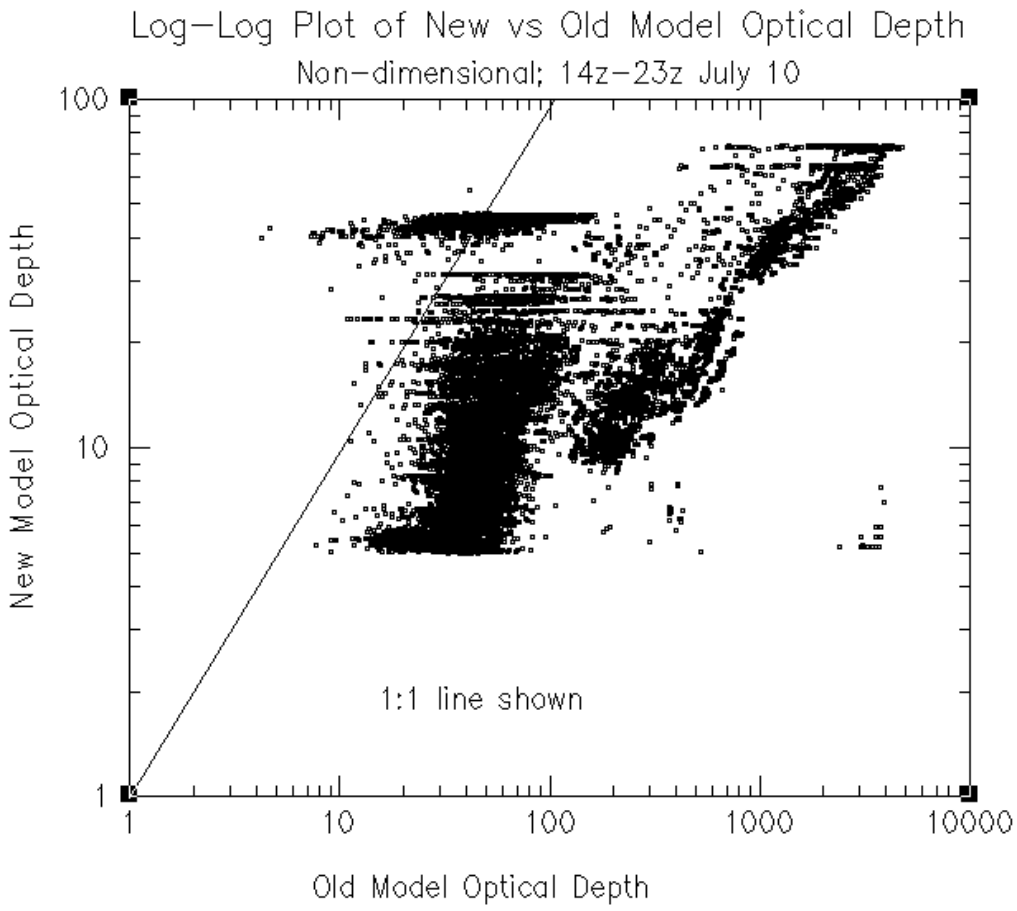

Figure 1. Log-Log plot showing optical depth calculations using the RADM (Chang, et al., 1987) formula, denoted “old,” and the Hansen (1983) formula, denoted “new,” for a wide-range of clouds calculated within the MAQSIP model as configured for the Seasonal Model for Regional Air Quality (SMRAQ) study.

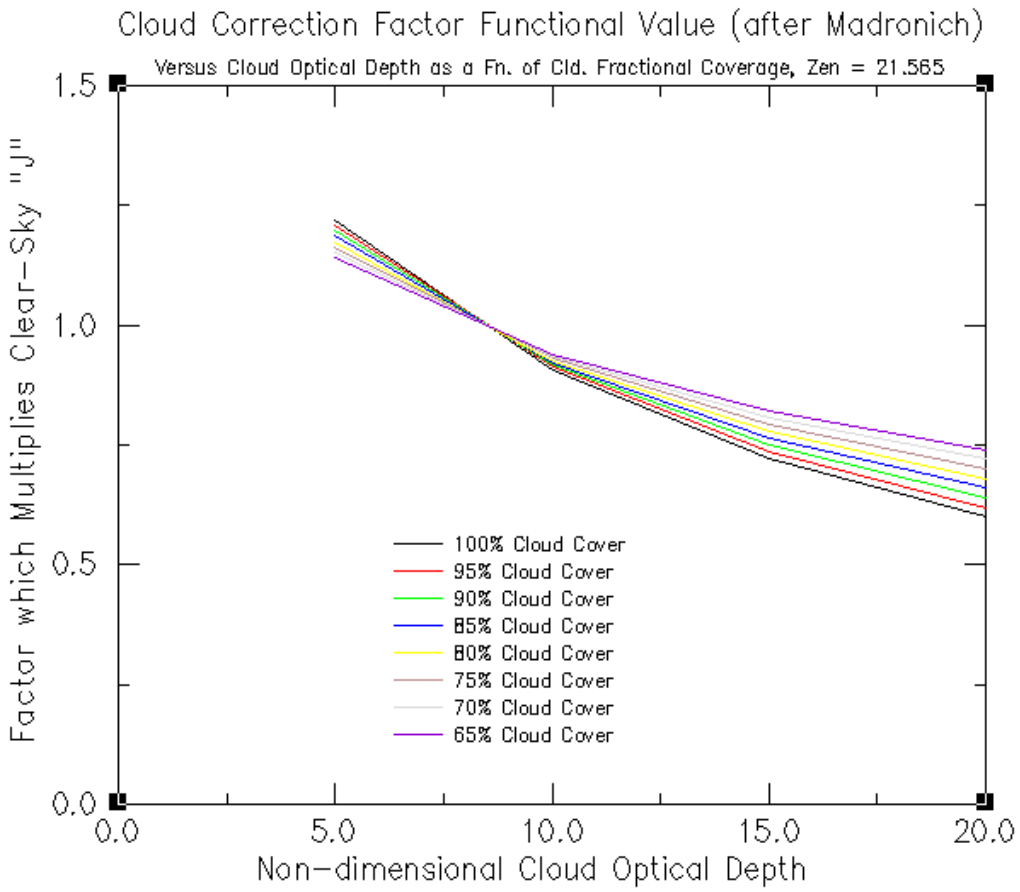

Figure 2. Behavior of below-cloud clear-sky “J” correction function published in Chang et al. (1987) and derived by S. Madronich for RADM, for optically thin clouds, as a function of cloud fractional coverage, for a solar zenith angle of 21.565 degrees.

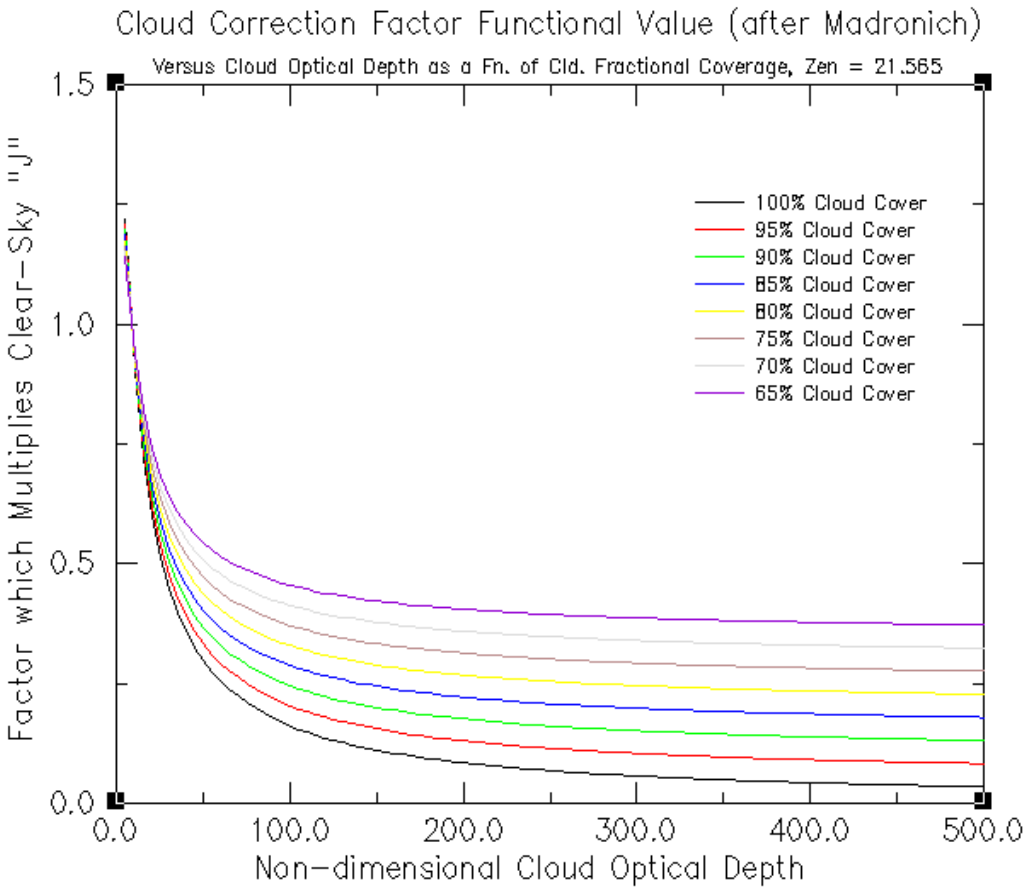

Figure 3. Same as in Figure 2, but for an optical depth range between 0 and 500.

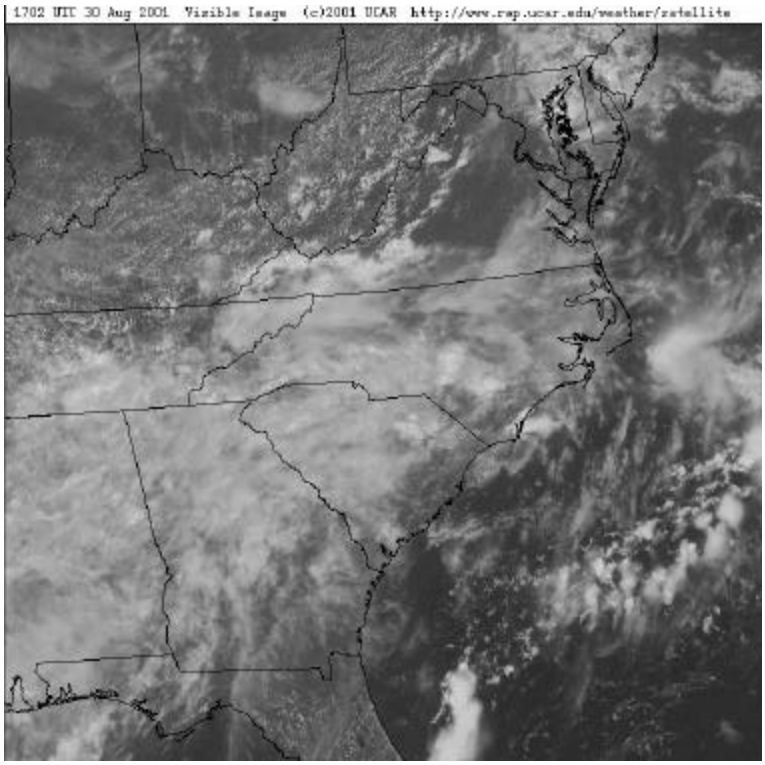

Figure 4. Visible satellite image valid 1700UTC, August 30, 2001, SE US

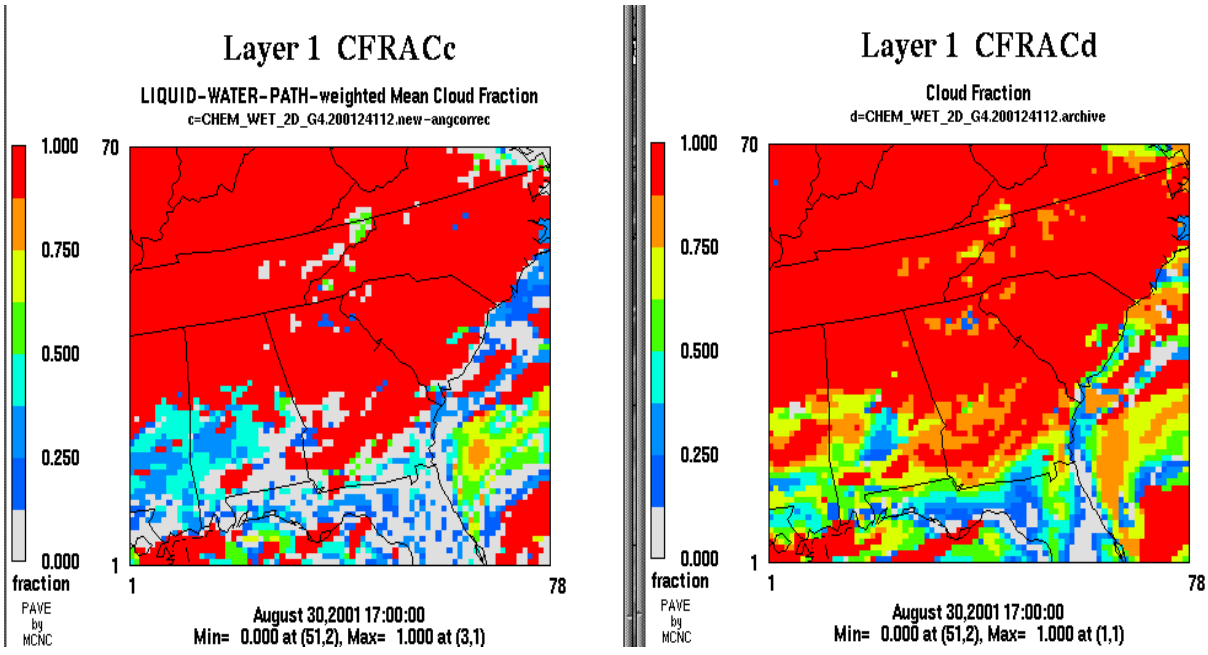

Figure 5. MM5/MAQSIP-RT predicted fractional cloud cover, 1700UTC, Aug. 30, 2001. *The new LWP-weighted fraction is on the left.*

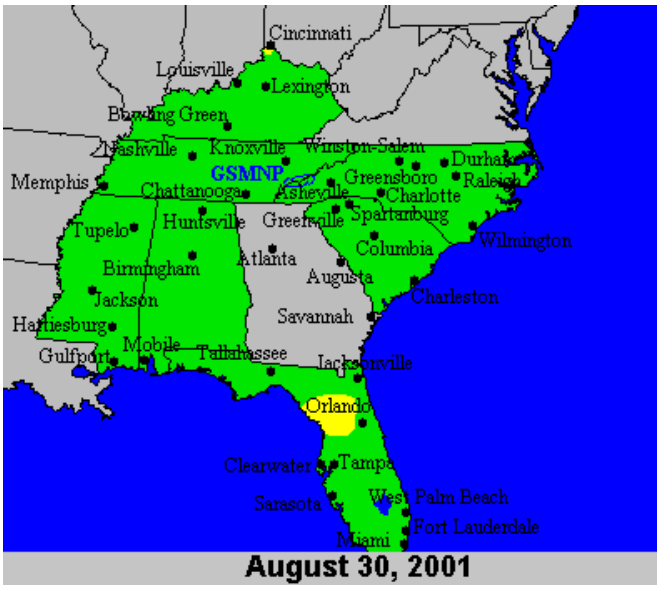

Figure 6. Peak 8-hour observed surface ozone concentrations, August 30th, 2001. (Courtesy US EPA AIRNOW map archive).

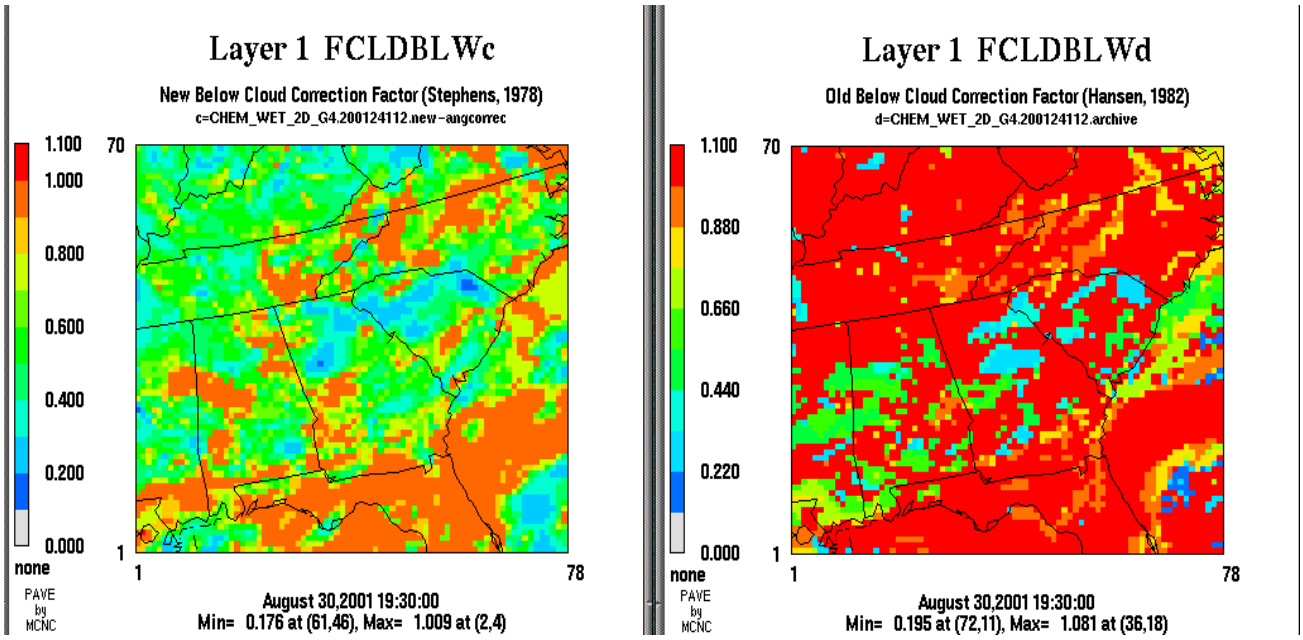

Figure 7. Below cloud "J" correction factor, 19:30UTC, August 30th, 2001. *MAQSIP-RT new is on the left, old on the right.*

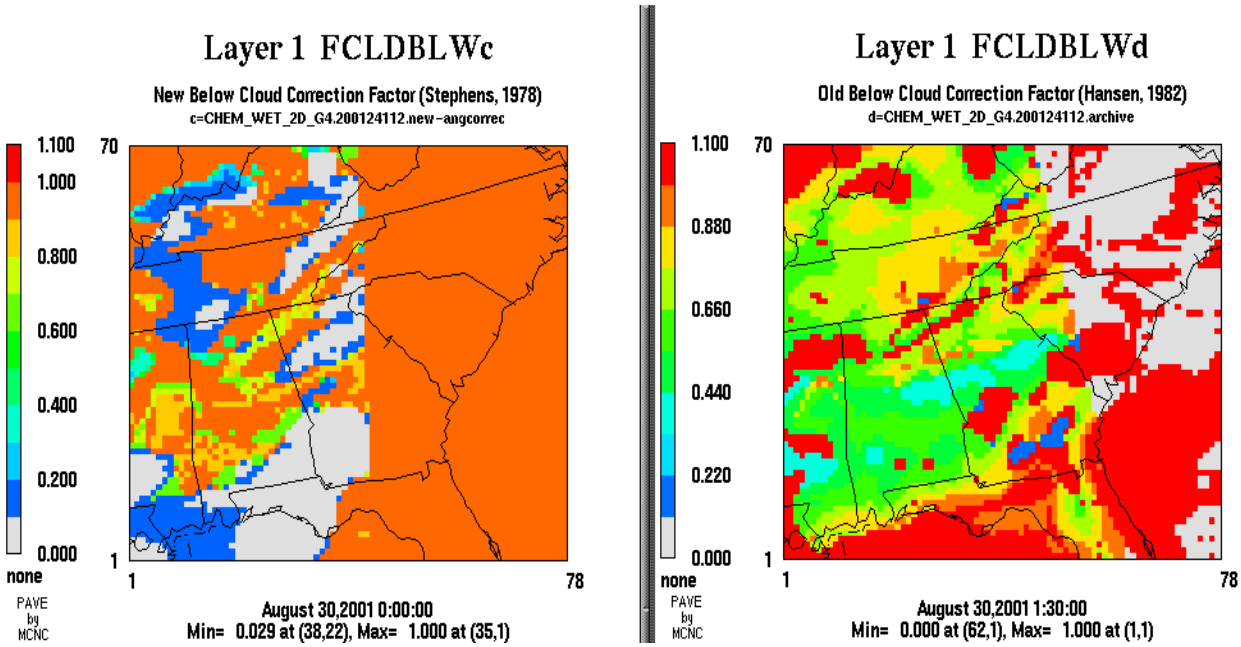

Figure 8. MAQSIP-RT modeled sunset on the evening of August 29th, 2001. The left hand figure shows the sunset line extending north-south from western NC south through the western tip of SC and through central Georgia. The line is obscured once it reaches Florida. Sunset is occurring at 00UTC August 30th (left-hand figure) along the indicated line. In the right-hand figure, the sunset line angles SSE through western NC and central SC, with sunset occurring at 0130UTC August 30th (right-hand figure), a full hour and a half late! *New model is on the left.*

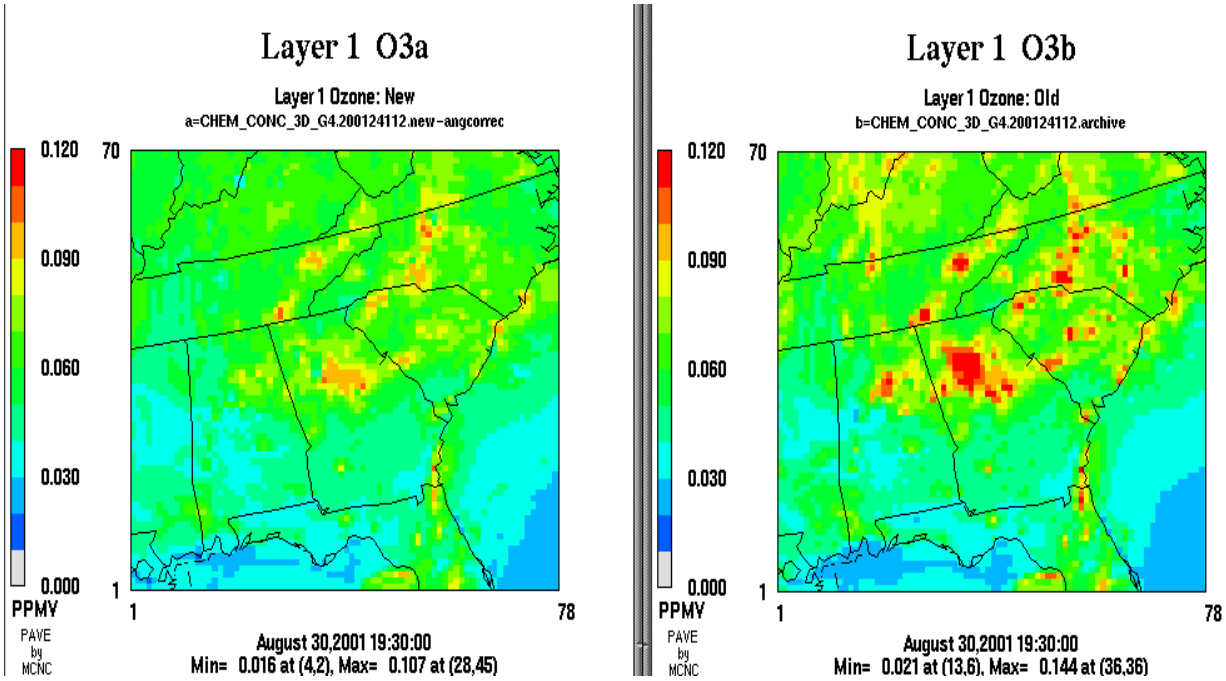

Figure 9. Forecast Ozone at 19:30UTC on August 30, 2001. *New model on the left, old model on the right.*

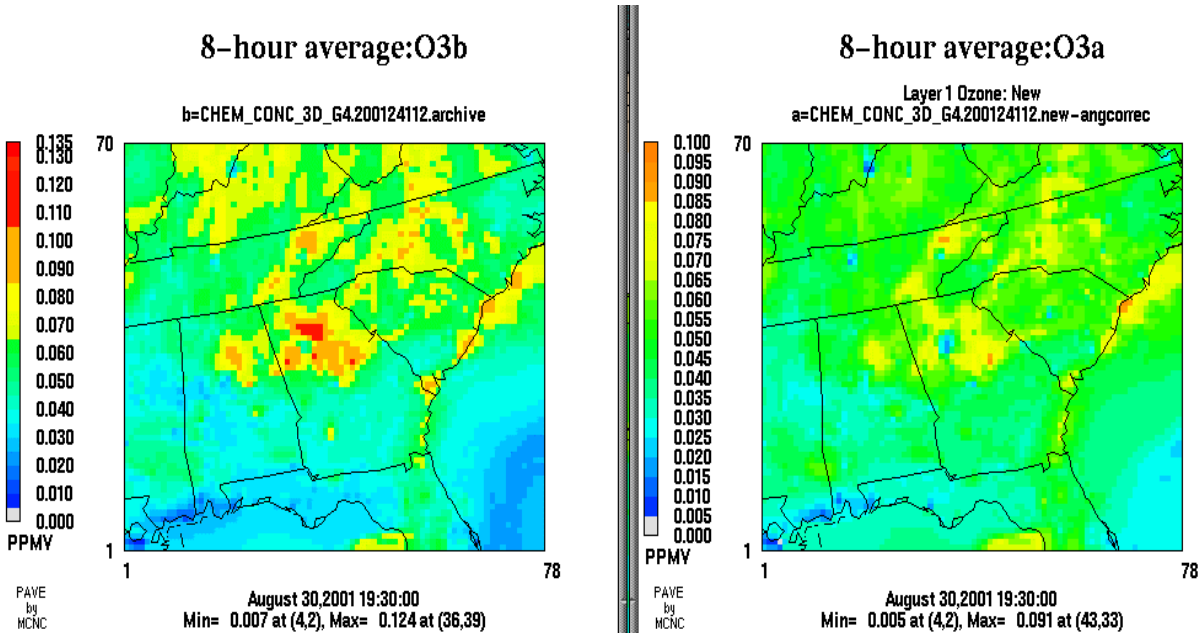

Figure 10. Forecast 8-hour average ozone (centered average) at 19:30UTC on August 30, 2001.
New model on the right, old model on the left.